

# Engine Hot Spots: Decay, Deflagration, Auto-Ignitive Propagation, or Detonation ?

L. Bates<sup>a</sup>, D. Bradley<sup>a</sup>, G. Paczko<sup>b</sup>, N. Peters<sup>b</sup>

<sup>a</sup>School of Mechanical Engineering, University of Leeds, UK, <sup>b</sup>Institute for Combustion Technology, RWTH Aachen, Germany.

## 1 Introduction

Reactive hot spots can arise for a number of reasons: partial mixing with hot gas or burned products, heat transfer from hot surfaces, and turbulent energy dissipation in flowing reactants. Their size may be of the order of millimetres. Following Zel'dovich [1], a gradient of reactivity can give rise to an auto-ignition velocity,  $u_a$ . At one extreme this can lead to a detonation, at another, to a benign controlled auto-ignitive propagation. The rate of change of the heat release rate at the hot spot determines the associated amplitude of the generated pressure pulse and, if  $u_a$  is high enough, to be close to the acoustic speed,  $a$ , this pulse can be coupled with the heat release in a detonation wave.

Earlier findings [2,3] from direct numerical simulations, DNS, of hot spot auto-ignitions in 0.5 H<sub>2</sub>/0.5 CO/air mixtures showed a peninsula could be constructed, within which detonations could develop. The boundaries were defined by dimensionless groups,  $a/u_a$ , and  $r_o/a\tau_e$ , in which  $r_o$  is the radius of a spherical hot spot and  $\tau_e$  is the excitation time, during which most of the heat release occurs at the end of the auto-ignition delay time [4]. This approach has been employed in studies of engine knock or super-knock in gasoline engines [5-9]. The phenomenon leading to super-knock is viewed as a sequence consisting of primary hot spots (pre-ignition) that initiate fuel conversion and heat release, followed by flame propagation which increases the pressure and thereby the temperature in the unburned part of the combustion chamber. In that part a secondary hot spot may subsequently occur, which may lead to a detonation according to the theory developed in [2,3]. While the latter process appears to be well understood, the mechanisms causing the primary hot spots are still subject of debate. The paper focuses on the secondary hot spots and the parameter range within which a detonation can develop.

The present paper extends these studies, focusing on secondary hot spots, by relating the detonation peninsula also to the activation energy of the mixture, and the temperature gradients at hot spots. This extended understanding is able to characterise engine auto-ignition over a wide range of conditions.

## 2 Auto-ignition in the strong ignition regime

The auto-ignition delay time at a given pressure is expressed by :

$$\tau_i = C \exp(E/RT), \text{ and} \quad (1)$$

$$\partial \tau_i / \partial T = \tau_i (E/RT^2). \quad (2)$$

The localised activation temperature,  $E/R$ , is expressed by :

$$\partial \ln \tau_i / \partial (1/T) = E/R, \text{ and} \quad (3)$$

the auto-ignition propagation velocity by

$$u_a = \partial r / \partial \tau_i = (\partial r / \partial T) (\partial T / \partial \tau_i). \quad (4)$$

Detonations are associated with the auto-ignitive front propagating at close to the acoustic velocity,  $a$ , and it is convenient to introduce the dimensionless ratio,  $\xi$  :

$$\xi = a/u_a = (\partial T / \partial r) (\partial \tau_i / \partial T) a. \quad (5)$$

A critical value of the temperature gradient, signified by suffix  $c$ , occurs when  $\xi = 1.0$ , and

$$(\partial T / \partial r)_c = (\partial T / a \partial \tau_i), \text{ with} \quad (6)$$

$$\xi = (\partial T / \partial r) (\partial T / \partial r)_c^{-1}. \quad (7)$$

For a given mixture and its conditions,  $\xi$  is proportional to  $\partial T / \partial r$ .

From Eqs. (2) and (5),

$$\xi = -\tau_i (E/RT^2) (\partial T / \partial r) a. \quad (8)$$

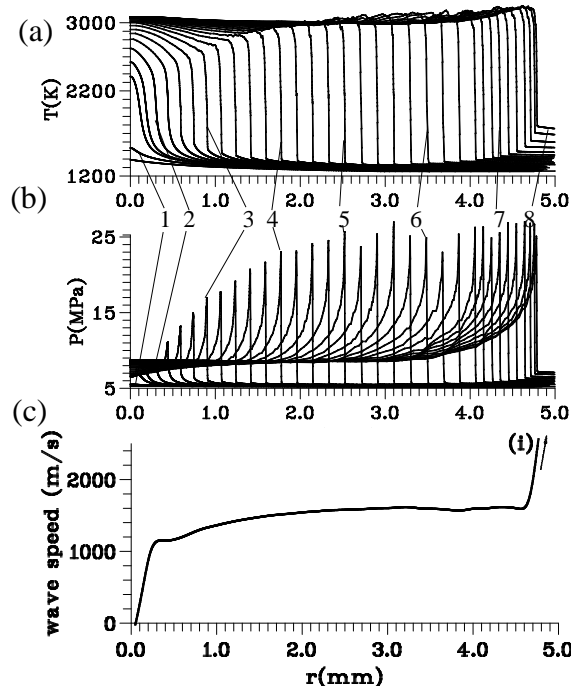


Figure 1. History of a hot spot,  $r_o = 3$  mm, with  $\xi = 1$ , stoichiometric 0.5 H<sub>2</sub>/0.5 CO/air,  $T_o = 1200$ K and  $P_o = 5.066$  MPa,  $\tau_i = 39.16$   $\mu$ s. Time sequence ( $\mu$ s) 1-35.81, 2-36.16, 3-36.64, 4-37.43, 5-37.72, 6-38.32, 7-38.86, 8-39.13. (a) temperature, (b) pressure, (c) combustion wave speed.

Both Voevodsky and Soloukhin [10] and Meyer and Oppenheim [11] used Eq. (2) to define the boundary between strong and weak auto-ignitions. Strong ignition was defined as a stable detonation, with near-instantaneous and uniform auto-ignition and a low value of the thermal diffusivity,  $(\partial\tau_i/\partial T)$ . Meyer and Oppenheim suggested a threshold value of  $\partial\tau_i/\partial T$  for this regime of  $-2 \mu\text{s/K}$ . Figure 1 shows results from the DNS studies of [2,3], for a detonation developing rapidly from a hot spot of radius 3 mm in a stoichiometric 0.5 H<sub>2</sub>/0.5 CO/air mixture with  $\xi = 1.0$  at 1200K,  $\tau_i = 39.16 \mu\text{s}$  and  $a = 731 \text{ m/s}$ . The temperature gradient across the hot spot was  $-2.426 \text{ K/mm}$  and thermal diffusivity  $-0.564 \mu\text{s/K}$ , smaller in magnitude than the Meyer and Oppenheim value of  $-2 \mu\text{s/K}$ . A hot spot developing to thermal explosion was also investigated in [2,3] with  $\phi = 0.75$  and at 1000K, which showed thermal diffusivity of  $-32 \mu\text{s/K}$ .

### 3 Excitation time and the detonation peninsula

The other relevant dimensionless group formulated in [2,3] is the time for the acoustic wave to move through the hot spot of radius  $r_o$ , divided by the excitation time and this is defined by  $\varepsilon$ :

$$\varepsilon = r_o / a \tau_e . \quad (9)$$

From Eq. (8)

$$\xi = -(\tau_i E / RT) (\partial T / T / \partial r / r_o) a / r_o . \quad (10)$$

Introducing  $\tau_e$ , gives

$$\xi \varepsilon = -\bar{E} (\partial \ln T / \partial \bar{r}), \text{ where} \quad (11)$$

$$\bar{E} = \frac{\tau_i}{\tau_e} \frac{E}{RT} \text{ and } \bar{r} = r / r_o . \quad (12)$$

If  $T_o$  is peak temperature at the centre of the hot spot,  $\partial \ln T / \partial \bar{r}$  can be approximated by  $\ln(T/T_o)$ . The associated error for an assumed constant linear gradient,  $\partial T / \partial r$ , ranges from 0.05% for  $\partial T / \partial r = -1 \text{ K/mm}$ , to 4.7% for  $-100 \text{ K/mm}$ .

Lee, Radulescu, Sharpe, Shepherd and co-workers [12-15] have demonstrated the importance of  $\bar{E}$  in assessing the stability of detonations. Low values of both  $E/RT$  and  $\tau_i/\tau_e$  are conducive to stability, with a spatially uniform structure, overlapping power pulses, and a reaction zone strongly coupled with the shock wave. These terms are coupled with  $\xi$  and  $\varepsilon$  in Eq. (10), through the driving hot spot temperature gradient [6,16].

Figure 2 shows plots of  $\xi$  against  $\varepsilon$  that define the peninsula, within which detonations can develop from hot spot auto-ignitions, and the other regimes. The peninsula was constructed from results of many simulations of hot spot auto-ignitions. The absence of turbulence was not unduly restrictive, as turbulence time scales can be about three orders of magnitude larger than the auto-ignition times. The simulations involved H<sub>2</sub>/CO/air mixtures [2,3], chosen because the detailed chemical kinetics were well established. The data for *n*-heptane/air and *i*-octane/air mixtures were subsequently simulated by Peters and Paczko. Data centred around respective values of  $\bar{E}$  of  $(110 \pm 67) 10^3$  at 1100K, and  $(15.6 \pm 8) 10^3$  at 1000K for H<sub>2</sub>/CO, and  $(2.45) 10^3$  at 800K for *n*-heptane and  $(58.7) 10^3$  at 893K for *i*-octane.

Although the different values of  $\bar{E}$  have but small influence upon the detonation peninsula boundaries, they influence the hot spot temperature elevation, through Eq. (11). If  $\bar{E}$  is known, the value of  $\partial \ln T / \partial \bar{r}$  then can be found at any point. Conversely, the maximum value of  $\partial \ln T / \partial \bar{r}$

might be designated, dependent upon the spatially distributed turbulent kinetic energy dissipation rate. When this is combined with the value of  $\bar{E}$  an operational point can be located on the  $\xi/\varepsilon$  diagram.

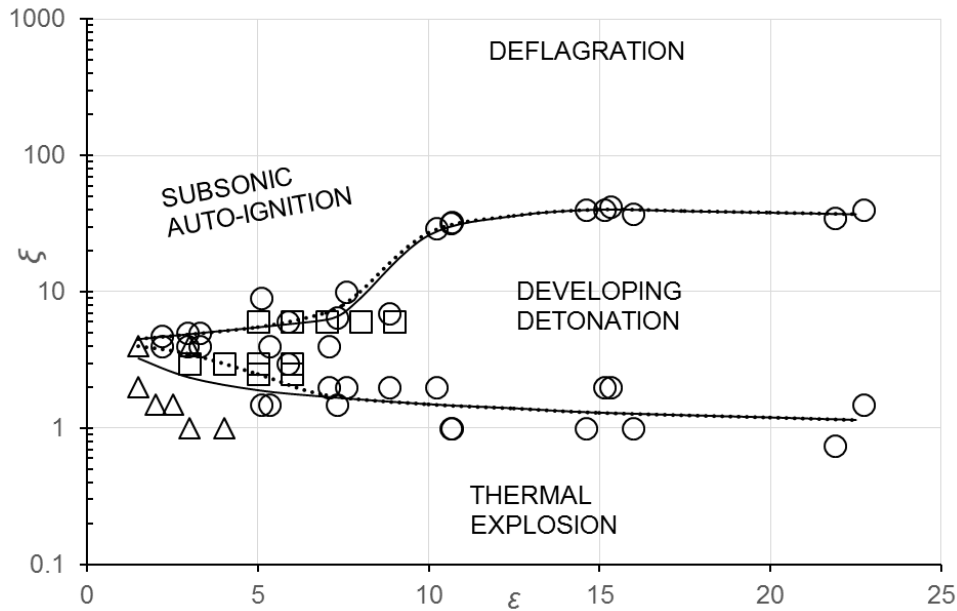


Figure 2.  $\xi/\varepsilon$  regime diagram,  $\text{H}_2/\text{CO}/\text{air}$  peninsula shown by dotted curves.  $\bigcirc$ :  $\text{H}_2/\text{CO}/\text{air}$  [4],  $\square$ :  $n\text{-C}_7\text{H}_{16}/\text{air}$ ,  $\Delta$ :  $i\text{-C}_8\text{H}_{18}/\text{air}$ .

#### 4 Engine performance and the detonation peninsula.

Table 1. Engine auto-ignition and super-knock conditions.

Engine	Fuel	Auto-ignitive mode	Fig. Ref.	$\phi$	$T$ K	$P$ MPa	$\bar{E}$	Ref.
1. Hydra single cylinder with Roots blower	PRF 84 [5,17,19]	Controlled benign MILD auto-ignition.	A	0.25	729	6.52	6,799	[18,6]
			B	0.25	811	4.84	543	
			C	0.25	1057	3.37	5,829	
2. Turbo-charged S.I. engine (GM Powertrain)	RON/MON 95/85, OI=105. Surrogate 0.62 <i>i</i> -octane, 0.29, toluene, 0.09 <i>n</i> -heptane, OI=105 [5]	No auto-ignition	D	1.0	800	7.0	13,269	[21]
		Fairly heavy knock	E	1.0	850	9.0	6,716	[21]
		Pre-ignition, super-knock	F	1.0	926	12.8	2,696	[21]
3. Turbo-charged S.I. engine (VW)	RON/MON 98/89, OI=107. Surrogate as above [5]	Pre-ignition, Super-knock	G	1.0	918	13.3	2,822	[22]
4. Turbo-charged S.I. engine (Tsinghua University, Beijing)	Composition in [24]. RON/MON, 94.1/81.9. Data for 93.4/81 from [5,18].	Slight knock	H	1.0	824	10.45	5,229	[23,24]
		Super-knock, deflagration	I	1.0	949	10.91	1,906	[23,24]
		Super-knock, detonation	J	1.0	917	10.5	2,467	[23,24]

A range of different engine auto-ignition conditions, covering four different engines, are reviewed and summarised in Table 1. The operational regimes are shown, relative to the developing detonation peninsula, and contours of  $\bar{E} \partial \ln T / \partial \bar{r}$ , on Fig. 3.

Conditions that are conducive to benign auto-ignitive burning are low burning velocities and temperatures just high enough for auto-ignition, such as lean combustion and with exhaust gas recirculation. The regime has been variously defined as one of controlled auto-ignition, flameless combustion, MILD combustion (moderate intense low-oxygen dilution). Conditions A to C on Fig. 3 are in this regime. The progression from no knock to super-knock is traced through the progressive blackening of the symbol. Condition D is representative of no knock, H represents slight knock, E heavier knock. F, G, I, and J represent super-knock, usually associated with auto-ignitive pre-ignition [25], with a subsequent strong developing detonation.

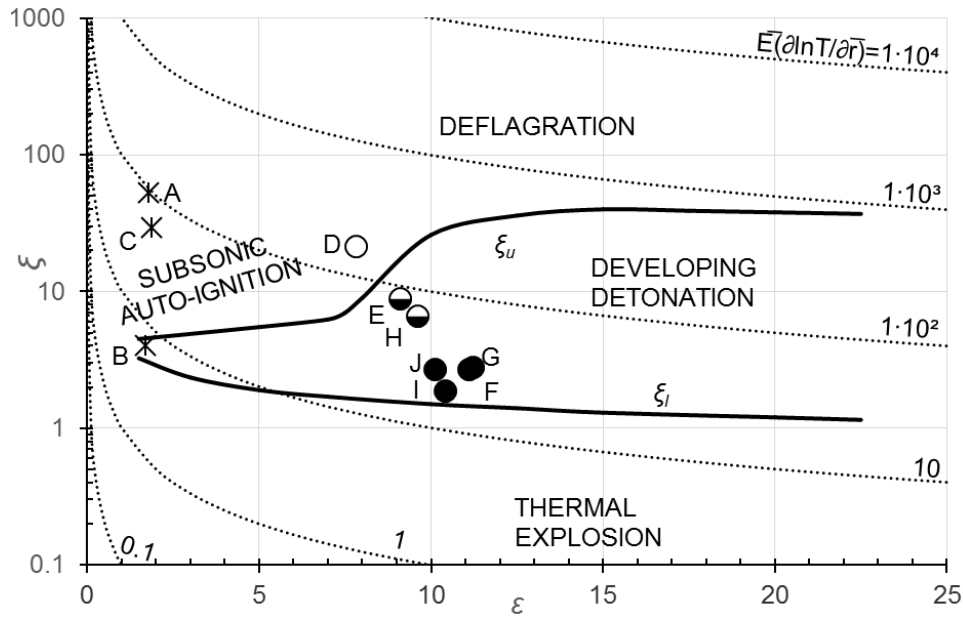


Figure 3. Increasing black fill of the symbols indicates increasing severity of knock for the different conditions in Table 1, from mild combustion to super-knock.

## 5 Conclusions

- i. The  $\xi$  and  $\varepsilon$  coordinates of the detonation peninsula are applicable over a wide range of fuels.
- ii. Knowledge of the  $\bar{E}$  parameter in Eq. (11) enables contours of hot spot temperature elevations to be inserted on the  $\xi / \varepsilon$  diagram, as on Fig. 3.
- iii. Such localised temperature elevations might arise from the dissipation of turbulent energy.
- iv. Regimes in which severe knock develops can be identified on the  $\xi / \varepsilon$  diagram.
- v. These can be translated into values of  $\tau_i$ ,  $\tau_e$ , and  $\bar{E}$ .
- vi. This approach avoids some of the problems of attempting to employ Octane Numbers outside their valid pressure, temperature, and fuel regimes, as discussed in [18], and suggests an alternative approach.
- vii. The super-knock regime on the  $\xi / \varepsilon$  peninsula corresponds to that for strong, stable, continuous detonations in ducts, also characterised by  $\xi$  close to unity, with low ( $\xi \varepsilon$ ),  $\bar{E}$ , and hot spot temperature elevations [6].

## Acknowledgement

Xin He is thanked for information on the fuel data for Engine 4.

## References

- [1] Zel'dovich YaB. (1980). Combust. Flame 39: 211-214.
- [2] Bradley D, Morley C, Gu XJ, Emerson DR. (2002): SAE paper 2002-01-2868, SP-1718 SAE International 2002 Powertrain & Fluid Systems Conference and Exhibition.
- [3] Gu XJ, Emerson DR, Bradley D. (2003) Combust. Flame 133 63-74.
- [4] Lutz AE, Kee RJ, Miller JA, Dwyer HA, Oppenheim AK. (1988) Proc. Combust. Inst. 22 1683–1693.
- [5] Kalghatgi GT, Bradley D, Andrae J, Harrison AJ. (2009) Internal Combustion Engines: Performance, Fuel Economy and Emissions, IMechE London, UK, 8-9 December 2009, Institution of Mechanical Engineers.
- [6] Bradley D. (2012) Phil. Trans. Royal Soc. A 370 689-714.
- [7] Rudloff J, Zaccardi JM, Richard S, Anderlohr JM. (2013) Proc. Combust Inst. 34 2959-2967.
- [8] Dai P, Chen Z, Chen S, Ju Y. (2014) Proc. Combust Inst. 35.
- [9] Peters N, Kerschens B, Paczko G. (2013) SAE paper 2013-01-1109.
- [10] Voevodsky VN, Soloukhin RI. (1965) Proc. Combust. Inst. 10 279-283.
- [11] Meyer JW, Oppenheim AK. (1971) Proc. Combust. Inst 13 1153-1164.
- [12] Radulescu MI, Ng HD, Lee JHS, Varatharajan B. (2002) Proc. Combust. Inst. 29, 2825–2831.
- [13] Short M, Sharpe GJ. (2003) Combust. Theory Modell. 7, 401–416.
- [14] Radulescu MI, Sharpe GJ, Law CK, Lee JHS. (2007) J. Fluid Mech. 580, 31–81.
- [15] Shepherd JE. (2009) Proc. Combust. Inst. 32 83–98.
- [16] Radulescu MI, Sharpe GJ, Bradley D. (2013) Proceedings of the Seventh International Seminar on Fire and Explosion Hazards, pp. 617-626, Research Publishing, Singapore. Eds. Bradley D, Makhviladze G, Molkov V, Sunderland P, Tamanini F.
- [17] Fieweger K, Blumenthal R, Adomeit G. (1997) Combust. Flame, 109 599-619.
- [18] Bradley D, Head RA. (2006) Combust. Flame 147 171-184.
- [19] Bradley D, Morley C, Walmsley HL. (2004) Proc. SAE Fuels and Lubricants Meeting, Toulouse.
- [20] Bradley D, Kalghatgi GT. (2009) Combust. Flame 156 2307-2318.
- [21] Rothenberger P. GM Powertrain, Germany, Private Communication [6].
- [22] Manz PW. VW Germany Private Communication [6].
- [23] Wang Z, Liu H, Song T, Qi Y, He X, Shuai S, Wang JX. (2014) Int. J. Engine Research.
- [24] Wang Z, Liu H, Song T, Xu Y, Wang JX. (2014) SAE 2014-01-1212.
- [25] Kalghatgi GT, Bradley D. (2012) Int. J of Engine Research 12(4) 399-414.